Effect of Swirl Ratio on In-cylinder Mixture *Distribution in Diesel Duel Fuel* Engine by Using CFD Analysis

Suleeporn Sombut[1], Krisada Wannatong[2], and Tanet Aroonsrisopon[1]
[1]Department of Mechanical Engineering, Faculty of Engineering, Kasetsart University, Bang Khen Campus
[2]Energy Application Technique and Engine Test Department,
PTT Research and Technology Institute, PTT Public Company Limited
Email: moey_31@hotmail.com, krisada.w@pttplc.com and tanet.a@ku.ac.th

Abstract

The current study examined use of swirl control valve in a diesel dual fuel (DDF) engine by using multi-dimensional CFD simulations. The engine conditions were under low load (approximately 30 N-m torque) operations at 1500 rpm. Results from steady flow simulations showed that using different open angles of the swirl flap provided different swirl ratios. Changes in the swirl ratio altered the mixture distribution in the cylinder. Results from engine flow simulations suggested that greater swirl ratios enhanced the mixing of the premixed methane-air mixture. The mixture became more uniformly distributed with narrower swirl flap angles. The more uniform mixture might lead to challenges in combustion control and hydrocarbon engine-out emissions.

Keywords

diesel dual fuel, CFD, swirl ratio, swirl flap, mixture distribution

Introduction

Natural gas (NG) was recognized as one of the promising alternative fuels for internal combustion engines [1]. It is now considered as one of the conventional fuels for transportations and industries in Thailand. In practice, mostly found in heavy-duty trucks in Thailand, a conventional diesel engine can be converted to a “dedicated” natural gas spark-ignition engine by reducing a compression ratio and replacing diesel injectors with spark plugs. An alternative way to fuel a diesel engine with natural gas is by means of using the modified *diesel dual fuel* (DDF) system. In a diesel dual fuel engine, natural gas is commonly injected into the intake ports and mixed with the air before drawn into the in-cylinder. In the compression process, premixed air-gaseous fuel mixture is compressed to a higher temperature and pressure slightly prior to top dead center (TDC). A small portion of diesel fuel is injected

at high pressure directly into the combustion chamber and reacts with the gas mixture, causing the ignition [2 - 4].

Moreover, the efficiency of an engine can be improved by increasing burn rate of fuel-air mixture [5]. This can be achieved in several ways, such as the design of the combustion chamber in order to reduce contact between the flame and the chamber surface, designed intake systems that impact a swirling motion to the incoming charge or use of the swirl control valve to enhance swirl in the combustion chamber [6]. The swirl ratio and the fluid motion can have a significant effect on fuel-air mixing, combustion, heat transfer, and emissions. Engine designs such as intake manifold, intake ports, cylinder head, piston, and, recently used in modern diesel engines, swirl control valves, affect the intake phenomena and in-cylinder flow fields [5].

Knowledge of air flow behaviors is particularly important for the development and optimization of intake port designs and combustion chamber designs. This knowledge can be obtained through flow measurement and multi-dimensional CFD analysis [7, 8]. This technique can be applied to both steady state and transient simulation. In contrast to steady state simulations, transient simulations have moving meshes for piston and valves. Thus a complete combustion cycle can be simulated [9, 10].

The current study investigated the use of swirl control valve installed at the intake port by using AVL-FIRE CFD simulation software. Our focus was on the in-cylinder mixture formation in a full 3-D grid. Since we only observed the mixture formation prior to the combustion, we ran the cold-flow simulation from the intake valve open to the end of the compression process.

It should be noted that the engine in this study was a four-cylinder turbocharger diesel engine. We simulated the condition if this engine was converted to operate in a premixed natural gas, diesel-ignited combustion mode. In this engine setup, natural gas was supplied through the multi-point port injection system (i.e. one injector for one cylinder). To reduce the computation time, our CFD model captured only the flow phenomena in one cylinder. Although this assumption did not consider the flow interaction between cylinders, it could lead us to examine effects of using swirl control valve on in-cylinder mixture distribution under different engine conditions. Interpretation from simulation results could lead to optimized combustion chamber modification for minimizing methane emissions.

Simulation Approach

The present work consisted of 1) steady flow simulations and 2) engine flow simulations. Descriptions for models and the mesh generation used in the current study are briefly provided as follows.

1. CFD Turbulence Model

The CFD technique approximates and numerically solves the fluid flow equations over the domain of interest, using a finite-volume mesh. The results of the iterative solution procedure may be conveniently manipulated and displayed graphically for analysis. In carrying out a CFD calculation it is necessary to follow a number of steps. With the AVL-FIRE

CFD solver, based on the finite volume approach, it allowed solving the equations of mass, momentum and energy conservation within each volume. The software offered several turbulence models depending on users' selection.

The state-of-the-art k-ζ-f turbulence model has been recently developed by Hanjalic *et al.* [11]. They proposed a version of eddy-viscosity model based on Durbin's elliptic relaxation concept [12]. The aim was to improve numerical stability of the original $\overline{V^2}/k$ model by solving a transport equation for the velocity scale ratio instead of the velocity scale $\overline{V^2}$ [13] is present in Eq. 1.

$$\zeta = \overline{V^2}/k \quad (1)$$

The k-ζ-f turbulence model was demonstrated for improvement of simulating unsteady flow characteristics. Also along with recommendation from AVL, we used the k-ζ-f turbulence model for all simulation in the present work.

2. Mesh Generation

The computational domain reproduced the actual geometry by 3D optical measurement, then created 3D model by reverse engineering.

This model used hexahedral cell. The computational domain composed of intake ports and valves, the cylinder and the piston bowl, as shown in Figure 1. The number of cells varied approximately from 500,000 cells (piston at top dead center: TDC) to 800,000 cells (piston at bottom dead center: BDC). Early during the intake valve open interval, meshes at intake seats were refined around the valve opening gap because this area was small and rapidly changed due to valve motion. During the middle phase of the intake stroke and during the compression stroke where the valve lift was greater, mesh size at valve opening gap became larger. As the intake valves were almost closed, the mesh size became smaller again. To avoid too small mesh size, the simulation considered the intake valves being closed if valve lifts were less than 0.6 mm.

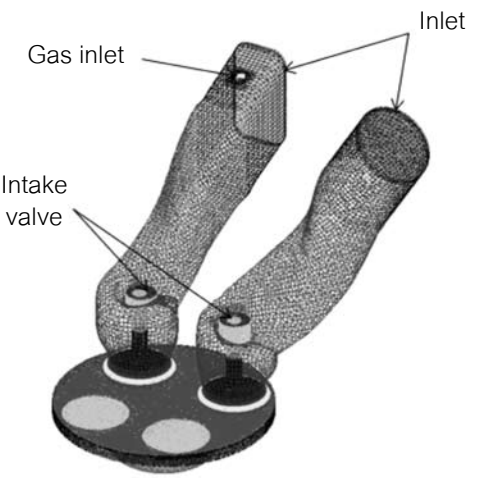

Figure 1 Computational mesh for the simulation

3. Engine Cycle Simulation

Data from experiments were used to calibrate engine cycle simulation models. In the present work, we used engine cycle simulation software package, namely AVL-BOOST [14]. Figure 2 shows the layout of the engine cycle model for a four-cylinder turbocharged Toyota 2KD-FTV diesel engine used in the current study. This AVL-BOOST model was from our previous work by Tepimonrat et al. [15]. Calculated mass flow profile, temperature and pressure of the charge mixture at each intake port were used as a boundary condition for CFD engine-flow simulations.

4. Case Description

The engine specifications are provided in Table 1. Natural gas was supplied to the engine by a sequential multi-point port natural gas injection system (i.e. one injector for one cylinder). The current study simulated the flow phenomena in cylinder 1 of this engine. The engine conditions were selected from available experimental data under low load (IMEP about 3 bar at cylinder 1 with the engine torque of approximately 30 N-m) at 1500 rpm.

Table 1 Engine specification

Engine model	Toyota 2KD-FTV
# Cylinder	4 cylinders, inline
Displaced volume	2,494 cc
Stroke	93.8 mm
Bore	92 mm
Connecting rod	158.5 mm
Compression ratio	18.5:1
Number of valves	16 valves (DOHC)
Exhaust valve open	30° BBDC (+150° after firing TDC)
Exhaust valve close	0° BTDC (+360° after firing TDC)
Inlet valve open	2° BTDC (+358° after firing TDC)
Inlet valve close	31° ABDC (-149° after firing TDC)

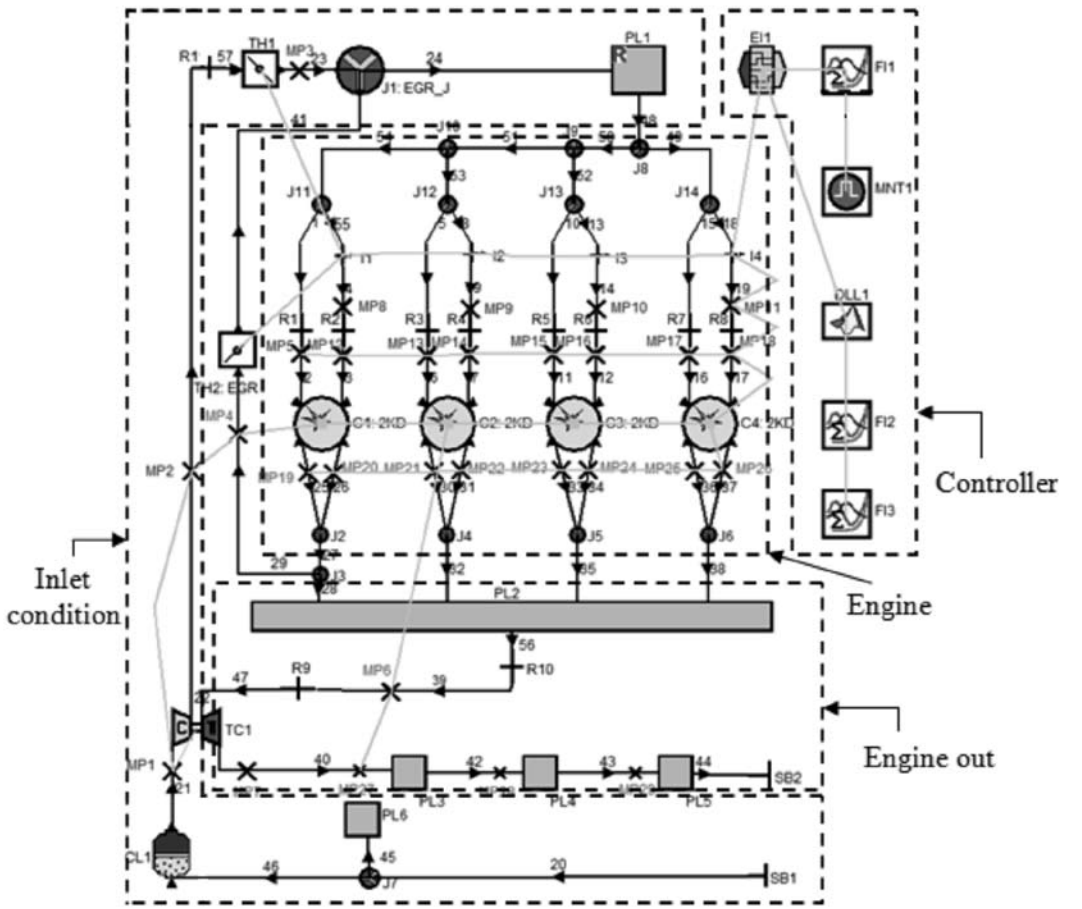

Figure 2 Engine cycle simulation model

4.1) Steady flow simulations

To accurately capture the physical geometry, as presented in the previous work by Pattarajaree *et al* [16], we adopted reverse engineering technique to generate CAD data for each engine component by using surface scanning. We combined the CAD data of each component and converted it to use in AVL-FIRE Work flow manager. As suggested in the AVL-FIRE theory [17], it is recommended to add a plenum at the inlet to mimic the flow field at the port entrance. Figure 3 shows the entire computational domain used in the current study. One can notice in this figure that each cylinder had two intake ports: the swirl port (a rectangular shape) and the round port (a circular shape). The swirl flap was installed at the entrance of the round intake port.

For the cylinder portion, a length of 2.5 times of the bore (230 mm) is recommended in order to avoid the influence of the outlet condition on the flow in the swirl measurement by a paddle wheel. To calculate the swirl ratio and the discharge coefficient, we added the AVL paddle wheel object, as shown in Figure 4, into the computational grid at the distance of 1.75 times of the bore (161 mm) below the cylinder head surface.

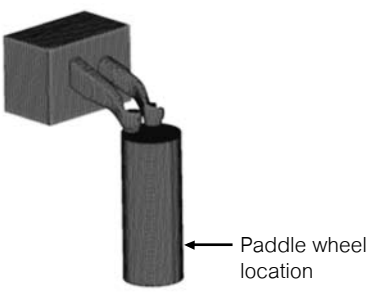

Figure 3 The computational domain for the steady flow simulations

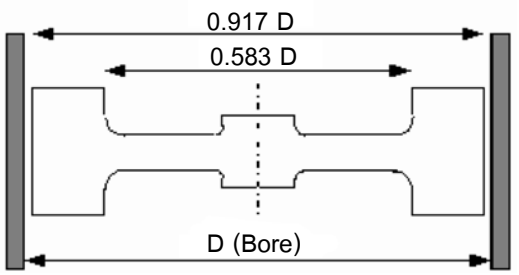

Figure 4 The AVL paddle wheel object in the model (AVL Inc, 2009)

The simulation conditions are listed in Table 2. For each condition, the position of intake valve was maintained constant. The static inlet pressure measured in experiments was used as a boundary condition. We ran simulations for three different positions of the swirl flap including 0o (ψ = 22°), 30° (ψ = 52°), 60° (ψ = 82°) and 80o (ψ = 102°) opening positions as shown in Figures 5. Note that the last opening position was the widest opening angle of this swirl flap.

Table 2 Engine conditions

Engine speed [rpm]	Torque [N.m]	Positions of the swirl flap (ψ)	Pressure inlet [bar]
1500	50	22°, 52°, 82°, 102°	1.0268

Figure 6 show the predictions of swirl ratios at different swirl flap positions. These swirl ratios were representations for the swirl ratio in the combustion chamber at intake valve closure (IVC). Figure 7 shows predicted discharge coefficients across each port (i.e. the CFD flow domains as shown). Based on these results, smaller opening angles of the swirl flap produced greater swirl ratios as one would expect. As the swirl flap opening angle

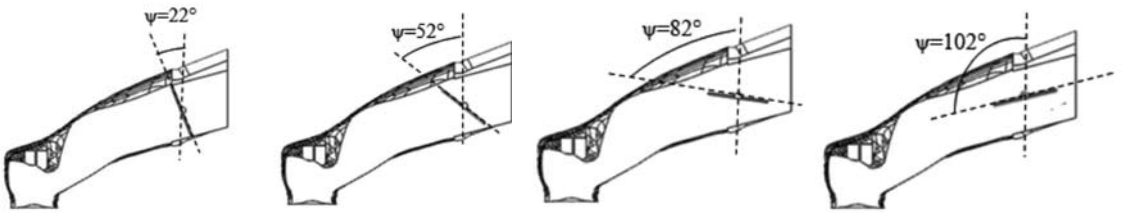

Figure 5 Position of swirl flap

was reduced, more portion of the intake mixture was forced to flow through the swirl port which enhanced the swirling motion of the cylinder charge. The more confined flow area, however, caused the flow discharge coefficient to decrease. The reduction in the discharge coefficient in the intake flow would penalize the volumetric efficiency and produce greater pumping loss of the engine.CFD data of predicted discharge coefficients across ports were imposed in the flow coefficient value at port elements in the AVL-BOOST engine cycle simulations. This was done to roughly capture trends of changes in the mass flows at each intake port as swirl flap opening positions changed. Figures 8 to 11 show predicted mass flow profiles from AVL-BOOST model. These data were used as inlet boundary conditions for the CFD engine flow simulations to examine the in-cylinder mixture formation.

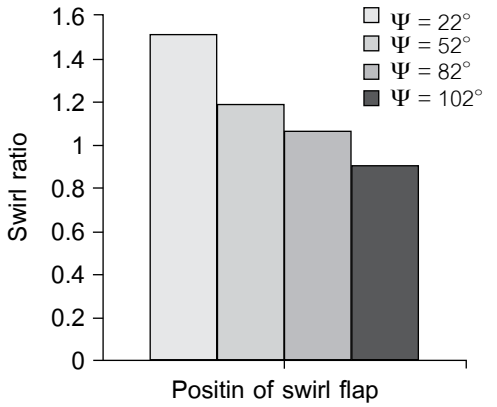

Figure 6 Predicted results of swirl ratios at IVC

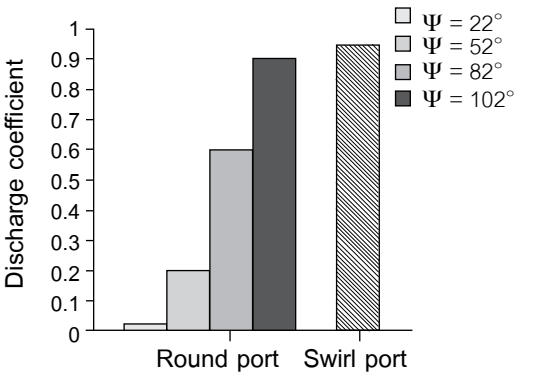

Figure 7 Predicted results of discharge coefficients across each port

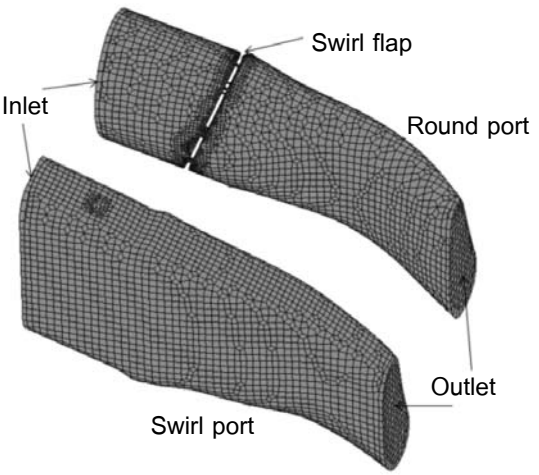

Figure 8 Mass flow profiles of the air-CH_4 mixture for the swirl flap at the fully closed position

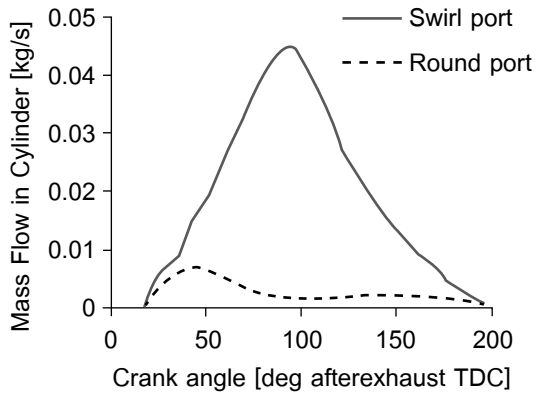

Figure 9 Mass flow profiles of the air-CH_4 mixture for the swirl flap at a 30° opening position

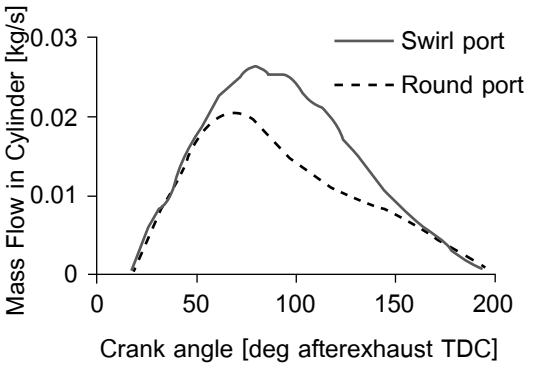

Figure 10 Mass flow profiles of the air-CH_4 mixture for the swirl flap at a 60° opening position

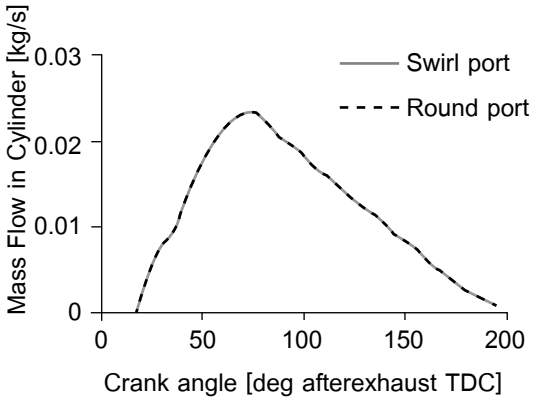

Figure 11 Mass flow profiles of the air-CH_4 mixture for the swirl flap at the fully opened position

4.2) Engine flow simulations

The calculation domain for engine flow simulations was the same as described above in Figure 3, but the entrance box was removed and the piston was added. Figure 12 shows the shape of the bowl-in piston obtained from reverse engineering. The start of simulation was at the exhaust TDC. The time step of 1°CA was used during the intake valve opening period and was decreased to be 0.2°CA when natural gas was injected into the swirl port. The amounts of natural gas injected were different depending on loads and speeds. Therefore, the injection duration was also different.

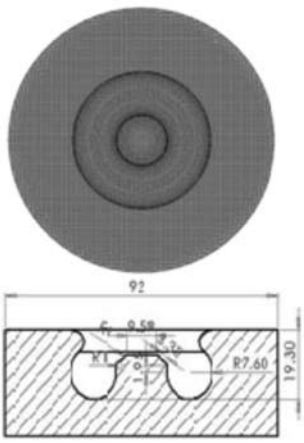

Figure 12 Schematic of a piston of the 2KD-FTV engine

Based on the engine conditions in Table 2, natural gas was injected between 33° and 360°CA. The surrogate model of natural gas was assumed to consist only of pure methane (CH_4). Figure 13 shows the mass flow profiles of CH_4 used as boundary conditions at the natural gas supply location. Turbulence kinetic energy was assumed to be 10% of the mean velocity. Similarly, the turbulence length

scale was also assumed to be 10% of hydraulic diameter in each cycle [5]. Temperature and pressure for the inlet sections were obtained from the engine cycle simulations.

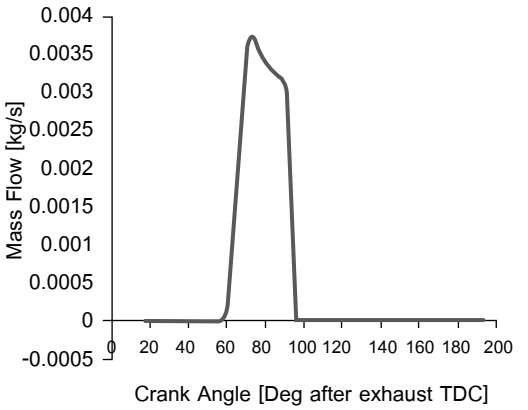

Figure 13 Mass flow profile of CH_4

5. Model validation

The current engine flow simulation model was validated by comparing the calculated cylinder pressure histories with the measured pressure histories. Figure 14 shows a comparison of the two pressure histories under 1500 rpm at the net IMEP of 3 bar with the swirl control valve being deactivated and activated. The current simulation could capture the measured pressure histories over the crank angle duration of interest very well. In this figure, the zero crank angle position was set at the compression TDC. For other figures to be discussed in the results and discussion section, the zero crank angle position was referred to the exhaust TDC for an easier observation of changes in the valve timings.

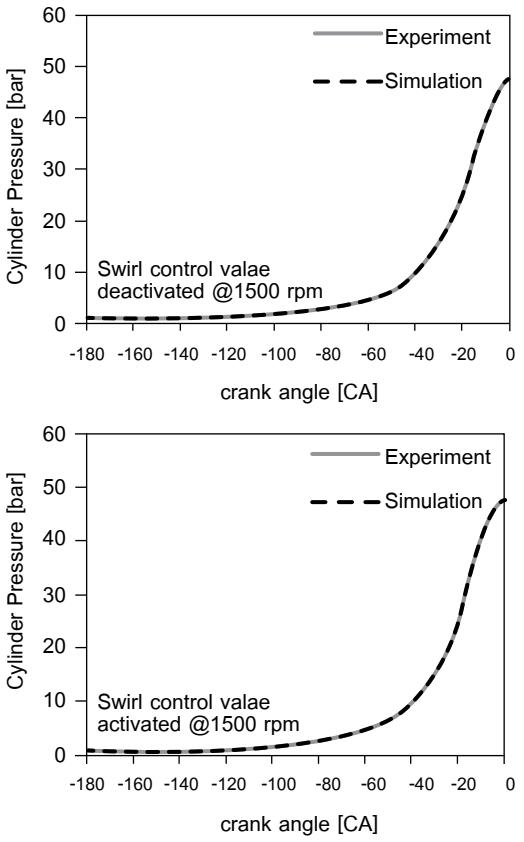

Figure 14 Cylinder pressure histories at 1500 rpm, net IMEP of 3 bars with the swirl control valve being deactivated and activated

Results and Discussion

In order to investigate the mixture distribution in the cylinder, we converted 3D results from AVL-FIRE into 2D format (r-θ coordinate). For each simulation case, groups of several computational cells were combined into small rings. Each ring was set at an equal radial width and an equal vertical thickness: dr = 1.53 mm and dh = 0.77 mm, respectively. The numbers of rings in the radial and the vertical directions are 30 and 50. These rings are grouped into 3 different zones in the cylinder,

Zone 1: the volume in the piston bowl (25% by vol.), Zone 2: the volume above the piston bowl (61% by vol.), and Zone 3: the cylinder wall area (14% by vol.). Note that Zone 3 consists of 20×3 rings at cylinder surface which are not moving according to cylinder movement shown in Figure 15. In order to obtain quantitative comparison, we compared the CH_4 mass for different zones relative to the total CH_4 mass in the entire combustion chamber.

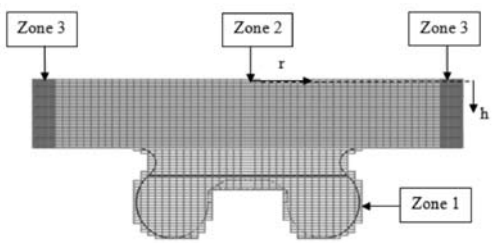

Figure 15 Zonal volume definitions

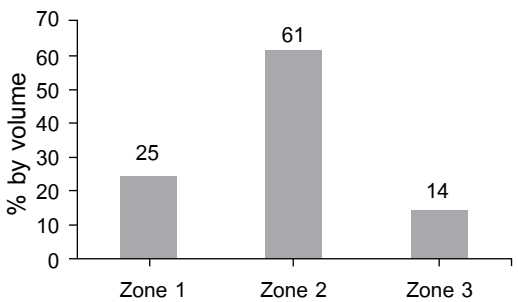

Figure 16 % by volume of zones

As shown in Figure 17, the TKE in all zones was increased with a smaller opening angle. The highest turbulence fluctuation was found in Zone 2 in all cases. The TKE in Zone 3 was smallest as it was closed to the wall regions.

Figure 18 shows the amount of CH_4 distribution in each zone. By observation at the fully open swirl-flap position, Zone 1 contained 24%, Zone 2 had 55%, and Zone 3 had 21% of CH_4 mass. This indicated that, together with percent by volume in each zone shown in Figure 16, there was greatest CH_4 concentration in the near-cylinder wall regions. As the swirl flap opening angle was narrower, the CH_4 concentration in each zone became more scattered. With greater turbulence kinetic energy, a stronger turbulence in the charge would enhance more mixing between the air and CH_4.

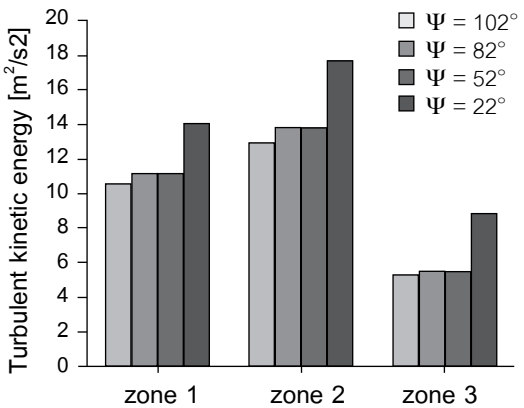

Figure 17 Turbulence kinetic energy of each zone

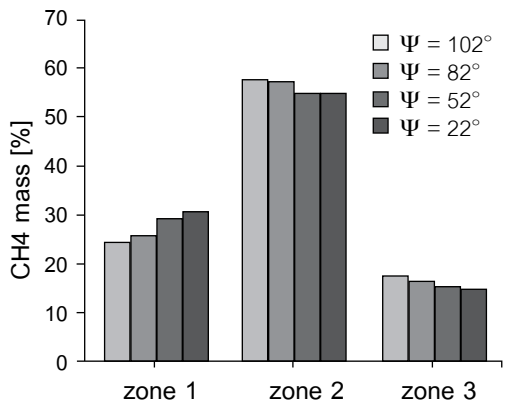

Figure 18 Methane distributions of each zone

To offer more insight into the mixing quality, one should take into account of the time evolution in the mixture formation process. In this sense, we looked at local CH_4

concentrations together with local vorticities on selected cut planes at the crank angle of 35° BTDC where the diesel injection was started. Figure 19 shows the two locations of the cut planes: section A-A was set around the middle of the squish height (approximately 6.4 mm away from the cylinder head) and section B-B was located at the largest diameter of the bore (approximately 22.8 mm away from the cylinder head).

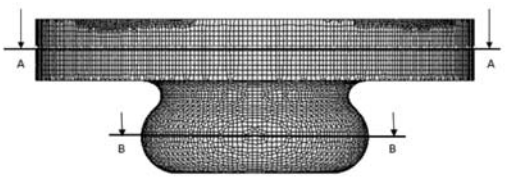

Figure 19 The location of the two cut planes

Data of contours of vorticities and mass fractions of methane are shown in Figure 20, 21. As the swirl flap angle was narrower, the area of high vorticities became larger in the bulk region. As a vorticity is an indication of high velocity gradient, a greater portion of high vorticities promoted more mixing in the bulk region. As a result, one can observe that the CH_4 distribution became more uniform with narrower opening angles of the swirl flap. This is consistent with our observation in Figure 17 where the distribution in the mixture concentration was more leveled.

As the mixture became more uniformly distributed with narrower swirl flap angles, it was not necessary to be beneficial for DDF operation. In fact, the more uniform mixture might lead to challenges in combustion control and hydrocarbon (HC) engine-out emissions [18]. Under low-load operation in a premixed charge compression ignition engine, partly stratified charge will be more prone to reach autoignition. Thus, it can improve the combustion stability and reduce HC and CO emissions of such an engine. Our future work is to examine the use of swirl control valve in DDF experiments. Data from simulations will help analyze the experiments using swirl control valve adjustment.

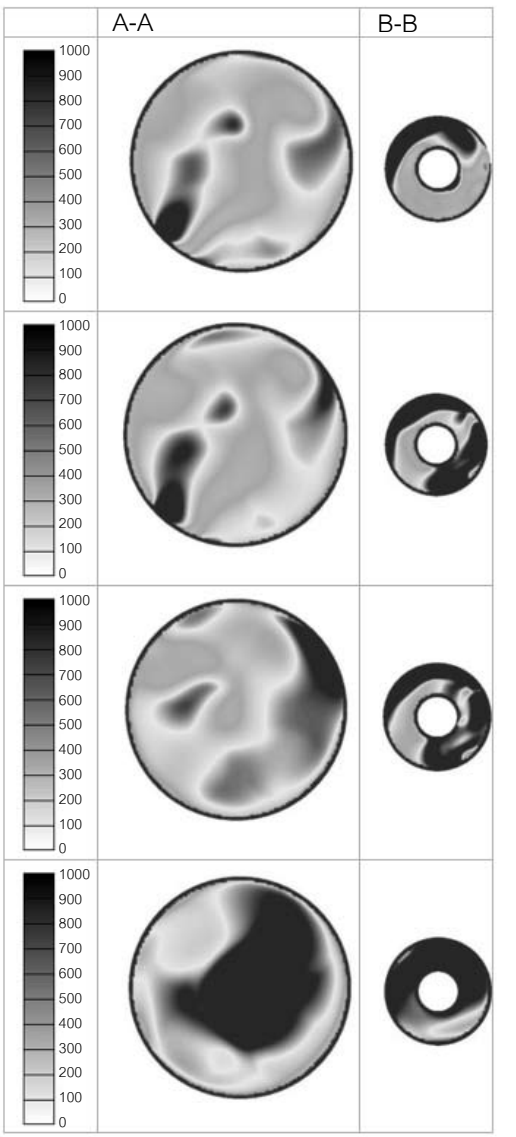

Figure 20 Contours of vorticity [1/S]

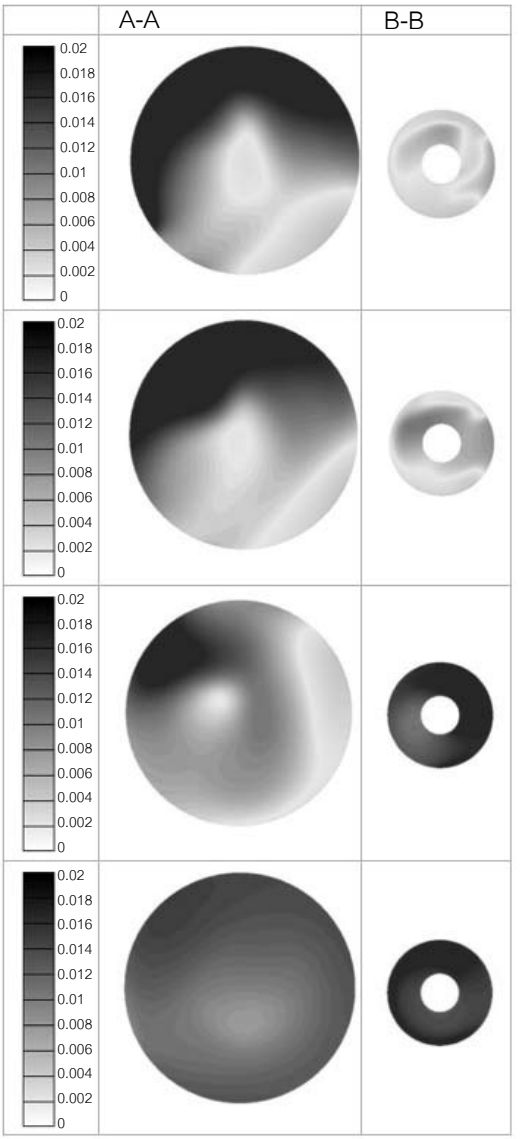

Figure 21 Contours of CH_4 mass fraction

Conclusion

The current study investigated the use of swirl flap installed at the intake port by using AVL-FIRE CFD simulation and the AVL-BOOST engine cycle simulation. The computational activities consisted of 2 parts: 1) steady-flow simulation to calculate the swirl ratio and discharge coefficients across the ports, and 2) the engine flow simulation to examine the in-cylinder mixture formation prior to the combustion for different opening angles of the swirl flap. The conclusions can be drawn as follows:

- Narrower opening angles of the swirl flap produced greater swirl ratios and lower discharge coefficients across the intake ports. This might lead to a more pumping work of the engine.
- With the swirl control valve deactivated, the premixed CH_4-air mixture had highest CH_4 concentration around the near-cylinder wall regions.
- Narrower opening angles of the swirl flap promoted turbulent kinetic energy and vorticity, causing the mixture distribution to become more leveled.

The findings from this study will help analyze the experiments using swirl control valve adjustment.

Acknowledgments

The authors would like to acknowledge the financial and technical support of PTT Public Company Limited (Thailand) and Kasetsart University (Thailand). We also acknowledge AVL LIST GmbH for granted use of AVL-FIRE and AVL-BOOST under the university partnership program.

References

[1] Aroonsrisopon, T., Salad, M., Wirojsakun, E., Wannatong, K., Siensanort, S., and Akarapan, N., 2009. "Injection Strategies for Operational Improvement of Diesel Dual Fuel Engines under Low Load Conditions", SAE paper 2009 - 01 - 1855.

[2] Singh , S., Krishnam, S.R., Srinivasan, K.K., and Midkiff, K.C., 2004. "Effect of Pilot Injection Timing, Pilot Quantity and Intake Charge Conditions on Performance and Emissions for an Advanced Low-Pilot-Ignited Natural Gas Engine", J. Engine Res, Issues 00404.

[3] Wannatong, K., Akarapanyavit, N., Siensanort, S., and Chanchaona, S., 2007. "Combustion and Knock Characteristics of Natural Gas Diesel Dual Fuel Engine", presented at SAE World Congress, 2007 - 01 - 2047.

[4] Wannatong, K., Akarapanyavit, N., Siensanort, S., Aroonsrisopon, T., and Chanchaona, S., 2009. "Injection New Diesel Dual Fuel Concepts: Part Load Improvement" SAE paper, 2009 - 01 - 1797.

[5] Ramadan, B., 2001. "A Study of Swirl Generation in DI Engines Using Kiva-3V",11th International Multidimensional Engine Modeling User's Group Meeting at the SAE Congress. U.S.A..

[6] Detao, L., Wang, Q., and Ping, L.J., 2002. "LDA Measurement and 3-D Modeling of Air Motion in Swirl Chamber of Diesel Engines", SAE paper 2002 - 01 - 0008.

[7] Greif, D., Berg, E. V., Tatschl, R., Corbinelli, G., D'Onofrio, M., 2005. "Integrated Cavitating Injector Flow and Spray Propagation Simulation in DI Gasoline Engine," SAE paper 2005 - 24 - 085.

[8] Maftouni, N. and Ebrahimi, R., 2006. "The Effect of Intake Manifold Runners Length on the Volumetric Efficiency by 3-D CFD Model," SAE paper 2006 - 32 - 0118.

[9] Tschöke, H., Naumann, B., Hartkopf, L., 2005. "Measurement and Simulation of Intake Port and In-Cylinder Air Flow of Diesel and Gasoline Engines," SAE paper 2005 - 24 - 072.

[10] Palumbo, M. F., 2007 " Measurement and Simulation of Intake Port and In-Cylinder Air Flow of Diesel and Gasoline Engines", SAE paper 2007 - 24 - 0047.

[11] Hanjalic, K., Popovac, M., and Hadziabdic, M. 2004. "A robust near-wall elliptic relaxation eddy-viscosity turbulence model for CFD," submitted to Int.J.Heat and Fluid Flow.

[12] Durbin, P.A., "Near-wall Turbulence closure Modelling without Damping Functions," Theor. Comput. Fluid Dyn. 3 (1991), pp. 1 - 13.

[13] AVL FIRE version 2009.1 User Guide, CFD Solver, 2009.

[14] AVL-BOOST version 2009.1 Users Guide, 2009.

[15] Tepimonrat, T., Kamsinla, K., Wirojsakun, E., Aroonsrisopon, T., and Wannatong, K., 2011. "Use of Exhaust Valve Timing Advance for High Natural Gas Utilization in Low-Load Diesel Dual Fuel Operation" SAE paper 2011 - 01 - 1767,

[16] Pattarajaree, E., Aroonsrisopon, T., and Wannatong, K. 2010. Effects of Piston Desige on In - cylinder Mixture Distribution in a Natural Gas Engine. J. of Research in Engineering & Technology, No. 7, 2010, pp. 5 - 20.

[17] AVL FIRE version 2009.1 Get Started Application Examples, 2009.

[18] Aroonsrisopon, T., Werner, P., Waldman, J.O., Sohm, V., Morikawa, T., Iida, M., and Foster, D.E., 2004. "Expanding the HCCI Operation with the Charge Stratification," Journal of Engines, SAE 2004 Transactions, Vol. 3, 2004 - 01 - 1756, pp.1130 - 1145.